Intrinsic relative magnetoconductivity of nonmagnetic metals

Yang Gao, Shengyuan A. Yang, and Qian Niu

Intrinsic Magnetoconductivity of Non-magnetic Metals

Yang Gao,[1] Shengyuan A. Yang,[2] and Qian Niu[1,3]

[1]*Department of Physics, The University of Texas at Austin, Austin, Texas 78712, USA*
[2]*Research Laboratory for Quantum Materials, Singapore University of Technology and Design, Singapore 487372, Singapore*
[3]*International Center for Quantum Materials, Peking University, Beijing 100871, China*

We present a theory of magnetoconductivity for general three-dimensional non-magnetic metals within the Berry-curvature-corrected semiclassical and Boltzmann framework. We find a new contribution, which is intrinsic in the sense that its ratio to the zero-magnetic-field conductivity is fully determined by the intrinsic band properties, independent of the transport relaxation time, showing a clear violation of Kohler's rule. Remarkably, this contribution can generally be positive for the longitudinal configuration, providing a new mechanism for the appearance of positive longitudinal magnetoconductivity besides the chiral anomaly effect.

I. INTRODUCTION

Magnetoconductivity, the field-dependent part of the diagonal component in the conductivity tensor: $\delta\sigma(B) \equiv \sigma(B) - \sigma_0$, where σ_0 is the conductivity under zero magnetic field, has long been a focus in solid-state physics due to its fascinating complexity and the rich information it could offer about the underlying electronic dynamics.[1,2] Depending on the relative orientation between the current flow and the magnetic field, the magnetoconductivity can be differentiated as transverse or longitudinal. While the magnetoconductivity under transverse configuration ($\boldsymbol{E} \perp \boldsymbol{B}$) can be naturally expected from the Lorentz force, the appearance of the magnetoconductivity under longitudinal configuration ($\boldsymbol{E} \parallel \boldsymbol{B}$) is a bit surprising, because at first look one expects that the electron's motion along the B-field should not be affected.[3]

In the high-magnetic-field regime ($\omega_c\tau \gg 1$, where ω_c is the cyclotron frequency and τ is the transport relaxation time), the electronic states are quantized into discrete Landau levels, for which the longitudinal magnetoconductivity can arise from the dramatic change in the states and the spectrum.[4,5] However, in the low-field *semiclassical* regime ($\omega_c\tau \ll 1$), where the external fields can be treated as perturbations to Bloch bands without Landau quantization, the mechanism for longitudinal magnetoconductivity is more subtle.

Indeed, in the simple Drude-Sommerfeld model for metals,[1] the longitudinal magnetoconductivity vanishes identically. One possible mechanism was identified in Ref. 6, arising due to certain special Fermi surface anisotropy. Recently, the interest in magneto-transport was further fueled by the discovery of topological semimetals.[7–11] Particularly, in the semiclassical regime, it was predicted that the chiral anomaly effect[12] associated with the topological band-crossing points can produce a positive longitudinal magnetoconductivity.[13] This generates great interest in the magneto-transport studies.[14–22] Experimentally, such positive signal was indeed observed in several doped topological semimetal candidates, and has been interpreted as compelling evidence for their topological band structures.[23,25–29,38]

For non-magnetic metals in the semiclassical regime,

due to the constraint of time reversal symmetry and Onsager's relation, $\delta\sigma(B) = \delta\sigma(-B)$, the leading order magnetoconductivity is of B^2, hence its theoretical formulation necessarily requires semiclassical equations of motion that are accurate to second order. However, previous theories (including Refs. 6 and 13) are based on semiclassical equations of only first-order accuracy, hence the obtained results are not complete. One naturally wonders: is there any important contribution missing from the picture? Meanwhile, peculiar positive longitudinal magnetoconductivity appears in recent experiments on several metallic materials.[30–32] These materials are not topological semimetals, and the possibility of anisotropic Fermi surface contribution is also ruled out in experiment, clearly pointing to the existence of new contributions missing in the previous theory.

Here, based on the recently developed semiclassical theory with second-order accuracy,[33,34] we formulate a theory of magneto-transport in non-magnetic metals for both transverse and longitudinal configurations in the semiclassical regime. We find that besides the previously obtained contributions, there is a new contribution to the magnetoconductivity that is linear in the transport relaxation time. We name it the intrinsic magnetoconductivity because its ratio to σ_0 is independent of scattering, only consisting of intrinsic band quantities including Berry curvature, orbital magnetic moment and so on. This intrinsic magnetoconductivity is generally nonzero regardless of the Fermi surface geometry, and it offers a new mechanism for the violation of Kohler's rule. Importantly, in systems without topological band-crossings and strong surface Fermi anisotropy, this contribution dominates the longitudinal magnetoconductivity, and furthermore, its sign could be positive, offering a new mechanism for positive longitudinal magnetoconductivity besides chiral anomaly.

Our paper is organized as follows. In Section II, we derive the magnetoconductivity based on the second-order semiclassical theory and the Boltzmann transport equation. In Section III, we analyze our main results and point out several important points. In Section IV and V, we apply our theory to two model examples. Especially, we demonstrate that a positive longitudinal magnetocon-

ductivity could result from the intrinsic magnetoconductivity in the semiclassical regime. Some discussion and our conclusion are presented in Section VI.

II. MAGNETOCONDUCTIVITY FROM SECOND ORDER SEMICLASSICAL THEORY

In the semiclassical theory, the Bloch electron dynamics is described by tracing the electron wave-packet center $(\boldsymbol{r}_c, \boldsymbol{k}_c)$ in the phase space.[35] Assuming the simple case where the Fermi level insects with a single band, the electric current can be expressed as

$$\boldsymbol{j} = -\int \frac{d^3k}{(2\pi)^3} \mathcal{D}\dot{\boldsymbol{r}}f \,, \qquad (1)$$

where $\mathcal{D}$ is a correction factor for the density of states,[36] and f is the distribution function. Here and hereafter, we set $e = \hbar = 1$ and drop the subscript c of the wave-packet coordinates.

As we mentioned, for non-magnetic metals in the semiclassical regime, the leading order contribution in $\delta\sigma(B)$ is of B^2. This means that we have to keep the third-order terms in the current (Eq. (1)) that are $\propto EB^2$. To this end, as we will show in a while, the following second-order semiclassical equations of motion are sufficient:[33]

$$\dot{\boldsymbol{r}} = \partial_{\boldsymbol{k}}\tilde{\varepsilon} - \dot{\boldsymbol{k}} \times \tilde{\boldsymbol{\Omega}} \,, \qquad (2)$$

$$\dot{\boldsymbol{k}} = -\boldsymbol{E} - \dot{\boldsymbol{r}} \times \boldsymbol{B} \,. \qquad (3)$$

Here $\tilde{\varepsilon}$ is the band energy including field-corrections up to second order,[34] $\tilde{\boldsymbol{\Omega}}$ is the modified Berry curvature including first-order field corrections. Due to the non-canonical structure of the equations of motion, the correction factor $\mathcal{D}$ in Eq. (1) takes the form $\mathcal{D} = 1 + \boldsymbol{B} \cdot \tilde{\boldsymbol{\Omega}}$.[33] It should be noted that although the semiclassical equations of motion are of a single-band form, the information of interband coherence is actually included through the geometrical quantities such as Berry curvature and orbital magnetic moment, which are indispensable for an accurate description of the Bloch electron dynamics.[35]

The remaining factor in in Eq.(1), i.e. the distribution function f, is typically solved from the Boltzmann equation. For a homogeneous system at steady state, it reads

$$\dot{\boldsymbol{k}} \cdot \frac{\partial f}{\partial \boldsymbol{k}} = \left.\frac{df}{dt}\right|_{\text{collison}} \,. \qquad (4)$$

Here $\dot{\boldsymbol{k}}$ can be substituted from Eq. (3), and the collision integral on the right hand side describes the relaxation due to the various scattering processes in the system. To proceed analytically, we take the relaxation time approximation such that the right hand side of Eq.(4) becomes $-(f - f_0)/\tau$, where f_0 is the equilibrium Fermi distribution and relaxation process is characterized by a single transport relaxation time τ. Note that in Eq.(4), the argument of the equilibrium distribution function f_0 must be the band energy including the magnetic field corrections, such that it guarantees a vanishing current at $E = 0$. Then the solution of the Boltzmann equation can be generally written as

$$f = \sum_{m=0}^{\infty} (-\tau\dot{\boldsymbol{k}} \cdot \partial_{\boldsymbol{k}})^m f_0(\tilde{\varepsilon}) \,. \qquad (5)$$

It is important to note that Eq.(5) does not imply an expansion in terms of τ. The solution to Boltzmann equation is expanded in terms of the external fields which are assumed to be small in the semiclassical regime. In contrast, we do not make any assumption on the value of the relaxation time.

Eqs. (2), (3), and (5) offer all the necessary and sufficient ingredients in evaluating the current in Eq. (1) to third order in external fields. To see this, one notes that since the equilibrium distribution f_0 does not contribute to the current, the factor f in Eq. (1) is at least of first order ($\dot{\boldsymbol{k}}$ in Eq. (5) is at least of first order according to Eq. (3)). Hence each of the other two factors $\mathcal{D}$ and $\dot{\boldsymbol{r}}$ in Eq. (1) only needs to be accurate to second order. This is why it is sufficient to have the Berry curvature $\tilde{\boldsymbol{\Omega}}$ in both $\mathcal{D}$ and $\dot{\boldsymbol{r}}$ to be corrected to first order and $\tilde{\varepsilon}$ in $\dot{\boldsymbol{r}}$ and f_0 to be corrected to second order.

Straightforward substitution and calculation yields the following contributions to the current up to third order (see Appendix A for details):

$$\boldsymbol{j}^{(a)} = -\tau^3 \int \frac{d^3k}{(2\pi)^3} \boldsymbol{v}_0(\boldsymbol{v}_0 \times \boldsymbol{B} \cdot \partial_{\boldsymbol{k}})^2(\boldsymbol{E} \cdot \partial_{\boldsymbol{k}})f_0(\varepsilon_0) - \tau \int \frac{d^3k}{(2\pi)^3}[\tilde{\boldsymbol{v}} + (\tilde{\boldsymbol{v}} \cdot \tilde{\boldsymbol{\Omega}})\boldsymbol{B}][\boldsymbol{E} + (\boldsymbol{E} \times \tilde{\boldsymbol{\Omega}}) \times \boldsymbol{B}] \cdot \partial_{\boldsymbol{k}}f_0(\tilde{\varepsilon}) \,. \qquad (6)$$

Here we group the various terms into two compact terms according to their τ dependence, ε_0 is the unperturbed band energy, $\boldsymbol{v}_0 = \partial_{\boldsymbol{k}}\varepsilon_0$ and $\tilde{\boldsymbol{v}} = \partial_{\boldsymbol{k}}\tilde{\varepsilon}$ are the band velocities for the unperturbed and perturbed band dispersions, respectively. Note that both terms here are Fermi surface contributions, i.e., carrying the derivative of the

Fermi distribution function. Hence the result can only be nonzero for a metal, and must vanish for insulators. We observe that the first term in Eq. (6) just recovers the contribution from Fermi surface anisotropy identified in Ref. 6, while the second term is new.

In addition, at second order, external fields induce a

shift $\delta\mu$ in the chemical potential (the linear-order correction vanishes as in usual first-order transport theory), which could lead to additional contributions to the current. Since $\delta\sigma_{xx} \sim B^2$, there are only two possible field-dependence in $\delta\mu$ that could contribute, $\delta\mu \sim EB$ or $\sim B^2$. The first possibility happens only with special band-crossings, i.e., in the chiral anomaly effect for doped Weyl semimetals.[13] In that case, the parallel E and B fields pump charges between a pair of Weyl points, shifting the chemical potential around each Weyl point in opposite ways. The current contributed from each Weyl point can be expressed as: $\boldsymbol{j}^{\mathrm{CA}} = \int \frac{d^3 k}{(2\pi)^3} \boldsymbol{B}(\boldsymbol{v}_0 \cdot \boldsymbol{\Omega}_0)\delta\mu f_0'$.[13] Here $\boldsymbol{\Omega}_0$ is the usual (unperturbed) Berry curvature, and $\delta\mu \propto \tau_v \chi \boldsymbol{E} \cdot \boldsymbol{B}$ where χ is the chirality of the Weyl point and τ_v is the intervalley scattering time that sustains the electron population imbalance between the pair of Weyl points.

The other possible contribution from $\delta\mu \sim B^2$ is more general, regardless of the band topology (see Appendix B for details). It yields the following current that contributes to the magnetoconductivity:

$$\boldsymbol{j}^{(b)} = \tau\delta\mu \int \frac{d^3 k}{(2\pi)^3} \boldsymbol{v}_0(\boldsymbol{v}_0 \cdot \boldsymbol{E}) f_0'' \,. \qquad (7)$$

The shift $\delta\mu$ can be fixed from the particle number conservation. For example, when the conduction band is separated from the valence band, the electron number n in the conduction band should be conserved. Under B-field, the shift $\delta\mu$ compensates the field correction of the band dispersion to ensure that $n = \int \frac{d^3 k}{(2\pi)^3} \mathcal{D} f_0(\tilde{\varepsilon} - \mu - \delta\mu)$ is a constant, from which we can solve out $\delta\mu$. Note that without E-field dependence, this shift $\delta\mu$ is an equilibrium property and is the same across the Brillouin zone.

This completes our general analysis for all possible contributions to the magnetoconductivity. Since we did not specify the directions of the fields, the result holds for both longitudinal and transverse magnetoconductivities.

III. ANALYSIS OF MAIN RESULT

For conventional metals (without chiral anomaly), the current up to third order is given by $\boldsymbol{j} = \boldsymbol{j}^{(a)} + \boldsymbol{j}^{(b)}$. One observes that the current at third order only has τ-dependence as $\sim \tau$ or $\sim \tau^3$. This is because τ is coupled with $\dot{\boldsymbol{k}}$ in Eq. (5), its power cannot exceed τ^3. Meanwhile, the term proportional to τ^2 is given by $-\tau^2 \int \frac{d^3 k}{(2\pi)^3}[\tilde{\boldsymbol{v}} + (\boldsymbol{v}_0 \cdot \boldsymbol{\Omega}_0)\boldsymbol{B}](\boldsymbol{v}_0 \times \boldsymbol{B} \cdot \boldsymbol{\partial_k})(\boldsymbol{E} \cdot \boldsymbol{\partial_k}) f(\tilde{\varepsilon})$, which is odd under time-reversal operation hence vanishes identically.

As mentioned, the first term in $\boldsymbol{j}^{(a)}$ recovers the result obtained in Ref. 6. It can be shown that its contribution to the transverse magnetoconductivity is always negative. For longitudinal configuration, its contribution is nonzero only when the Fermi surface has special anisotropy.[6]

Besides recovering the previously known contributions, most importantly, we discover new contributions, including $\boldsymbol{j}^{(b)}$ and the second term in $\boldsymbol{j}^{(a)}$. These terms only appear when using a complete second-order semiclassical theory, hence they are missing in previous works. Due to their common τ-linear dependence, we combine the two terms together, and name their resulting contribution to $\delta\sigma$ as the intrinsic magnetoconductivity ($\delta\sigma^{\mathrm{int}}$), because the ratio $\delta\sigma^{\mathrm{int}}/\sigma_0$ is independent of τ, consisting entirely of intrinsic band quantities (apart from the B^2 factor).

Our result has important implications on Kohler's rule.[2] Kohler's rule states that the ratio $\delta\sigma/\sigma_0$ depends on the B-field through the quantity $\omega_c\tau$. Since $\sigma_0 \propto \tau$, samples with different relaxation times can be related by plotting the ratios against a rescaled field $B\sigma_0$: $\delta\sigma/\sigma_0 = F(B\sigma_0)$. Kohler's rule can be derived in the first-order semiclassical theory by assuming a single species of charge carriers and a single relaxation time. Any deviation from Kohler's rule is usually interpreted as from factors beyond the semiclassical description or from the presence of multiple types of carriers or multiple scattering times.[40] Here, we see that the first term in $\boldsymbol{j}^{(a)}$, which is previously obtain from first-order semiclassical theory, indeed obeys Kohler's rule. Denoting its contribution to the magnetoconductivity as the extrinsic one $\delta\sigma^{\mathrm{ext}}$, we have $\delta\sigma^{\mathrm{ext}}/\sigma_0 \sim (\omega_c\tau)^2$. However, the new intrinsic contribution clearly violates Kohler's rule because $\delta\sigma^{\mathrm{int}}/\sigma_0$ is independent of τ. Instead, we may regard $\delta\sigma^{\mathrm{int}}/\sigma_0 \sim (\omega_c\tau_b)^2$ by replacing τ with another intrinsic time scale $\tau_b = \hbar/\varepsilon$, where ε is an intrinsic energy scale such as the band gap or the chemical potential. Since our theory is within the semiclassical framework and under the same conditions on carrier type and relaxation time, it represents a new mechanism for the violation of Kohler's rule. Hence, the validity of Kohler's rule would need the intrinsic contribution to be insignificant compared with the extrinsic one. This could happen at least for two cases: (i) due to their different τ-dependence, $\delta\sigma^{\mathrm{ext}}$ generally dominates over $\delta\sigma^{\mathrm{int}}$ in clean samples where τ is large; (ii) since $\delta\sigma^{\mathrm{int}}$ depends on nontrivial geometrical quantities such as Berry curvature and orbital magnetic moment, it becomes insignificant when these quantities are small on the Fermi surface.

Another important consequence of the intrinsic contribution is that it offers a new origin of the peculiar longitudinal magnetoconductivity. Compared with the chiral anomaly contribution, they both depend on geometric quantities such as the Berry curvature, but chiral anomaly contribution requires the special Weyl-point band structure, whereas the intrinsic contribution does not have this restriction—it can be present for conventional metals. Consequently, for systems with relatively isotropic Fermi surfaces and without Weyl points, the intrinsic contribution can dominate the longitudinal magnetoconductivity. As illustrated in the following examples, it can be quite sizable for bands with nonzero Berry curvatures and orbital magnetic moments, and more remarkably, it can be positive. Therefore, our theory provides a new mechanism for positive longitudinal magnetoconductivity in conventional metals.

IV. EXAMPLE I: WEYL SEMIMETAL

In the following, we apply our theory to two concrete examples. In the first example, we consider the low-energy model of a doped Weyl semimetal. Near the Fermi energy, Weyl semimetals have isolated Weyl points, each described by a Weyl Hamiltonian: $H = \chi v_F \boldsymbol{k}\cdot\boldsymbol{\sigma}$, where $\boldsymbol{\sigma}$ is the vector of Pauli matrices denoting the two crossing bands, $\chi = \pm 1$ gives the chirality, and v_F is the Fermi velocity. When time reversal symmetry is preserved, there are at least two pairs of Weyl points in the Brillouin zone.

Consider electron-doped case with $\mu > 0$, and assume that the B-field is along the z-direction. With two pairs of Weyl points, we find that the intrinsic magnetoconductivity is given by (see Appendix C for details)

$$\delta\sigma_\parallel^{\text{int}} = \frac{2}{15}\sigma_0(\omega_c\tau_b)^2\,, \qquad \delta\sigma_\perp^{\text{int}} = -\frac{17}{30}\sigma_0(\omega_c\tau_b)^2\,, \quad (8)$$

for longitudinal and transverse configurations respectively. Here the zero-magnetic-field conductivity $\sigma_0 = 2\mu^2\tau/(3\pi^2 v_F)$, $\omega_c = v_F^2 B/\mu$, and $\tau_b = 1/\mu$ is the Fermi time scale. One observes that the intrinsic magnetoconductivity takes different signs for the two configurations, and more importantly, the intrinsic longitudinal magnetoconductivity can be positive.

In comparison, the extrinsic contribution as from the first term in $\boldsymbol{j}^{(a)}$ is given by

$$\delta\sigma_\parallel^{\text{ext}} = 0\,, \qquad \delta\sigma_\perp^{\text{ext}} = -\sigma_0(\omega_c\tau)^2\,. \quad (9)$$

Here $\delta\sigma_\parallel^{\text{ext}}$ is zero because the Fermi surface is isotropic, whereas $\delta\sigma_\perp^{\text{ext}}$ is nonzero and follows Kohler's rule as expected.

Finally, in Weyl semimetals, there is a positive longitudinal magnetoconductivity from the chiral anomaly effect $\delta\sigma_\parallel^{\text{CA}}$. It is interesting to consider the ratio between the intrinsic contribution and the chiral anomaly one:

$$\frac{\delta\sigma_\parallel^{\text{int}}}{\delta\sigma_\parallel^{\text{CA}}} = \frac{8}{45}\frac{\tau}{\tau_v}\,. \quad (10)$$

We observe that it only depends on the ratio between the two relaxation times. Generally, the intervalley scattering time τ_v is much larger than τ,[17] so in doped Weyl semimetals, the chiral anomaly contribution is more important than the intrinsic contribution for the positive longitudinal magnetoconductivity.

When transverse and longitudinal magnetoconductivities are of different signs, for each B-field strength, by changing the mutual orientation between E-field and B-field, there exists a critical angle θ_c between the two fields at which the magnetoconductivity changes sign. Using the result obtained above, we find that the critical angle for this simple Weyl model is given by

$$\theta_c(B) = \text{arccot}\frac{34 + 60(\omega_c\tau)^2}{8 + 45(\tau_v/\tau)}\,. \quad (11)$$
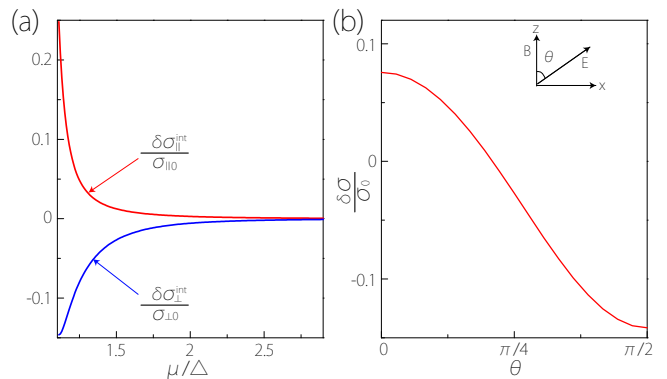

FIG. 1. (a) Intrinsic magnetoconductivities for model (12) versus the chemical potential. Here $\sigma_{\perp 0}$ and $\sigma_{\parallel 0}$ are zero-magnetic-field conductivities under transverse and longitudinal configurations respectively. (b) Ratio between magnetoconductivity $\delta\sigma$ and zero-magnetic-field resistivity σ_0 versus the angle θ between E and B fields, as illustrated in the inset. Here the model parameters are chosen as $B = 2$T, $\Delta = 50$meV, $v_F = 9.2 \times 10^5$m/s, and $m^* = 0.1m_e$ (m_e is the free electron mass). In (b) we take $\mu = 60$meV.

The point is that although here the intrinsic contribution to the longitudinal magnetoconductivity is relatively small, its contribution to the transverse magnetoconductivity can be important provided that τ_b/τ is sizable. Hence the intrinsic contribution must be included in estimating the critical angle.

V. EXAMPLE II: METAL WITHOUT BAND-CROSSING

In the second example, we consider a two-band model without any band-crossing point. It has two valleys in the Brillouin zone connected by time reversal symmetry

$$H_\chi = \chi v_F k_x \sigma_x + v_F k_y \sigma_y + \left(\Delta + \frac{k_z^2}{2m^*}\right)\sigma_z. \quad (12)$$

Here $\chi = \pm 1$ labels the two valleys, v_F, Δ, and m^* (assumed to be positive) are model parameters, and the pseudospin σ_i here denotes the two-band degree of freedom. The two bands are separated by a gap of 2Δ. Such a continuum model can be derived from a lattice model, e.g., defined on a 3D lattice consisting of 2D honeycomb lattices AA-stacked along the z-direction (see Appendix D for details).

Consider the electron-doped case with $\mu > \Delta$ and take the B-field to be along the z-direction. For longitudinal magnetoconductivity, it is clear that there is no chiral anomaly contribution since there is no Weyl point. And because of the axial symmetry of the Fermi surface, the extrinsic contribution $\delta\sigma_\parallel^{\text{ext}}$ also vanishes. The only nonzero contribution here is the intrinsic one, and we find that it gives a positive longitudinal magnetoconductivity, as illustrated in Fig. 1(a). From the figure, we observe that the magnitude of the intrinsic magnetoconductivity

decreases as μ increases. It is because the intrinsic contribution is a Fermi surface property that highly depends on the geometric quantities such as Berry curvature and orbital magnetic moment, which are concentrated near the band edge in this model.

In Fig. 1(b), we plot the magnetoconductivity containing both intrinsic and extrinsic contributions against the orientation of the E-field. Here B-field is taken to be fixed along the z-direction, and θ is the angle between the fields. One observes that the magnetoconductivity gradually changes from positive in the longitudinal case to negative in the transverse configuration, indicating that the magnetoresistivity changes from negative to positive in the process.

VI. DISCUSSION AND CONCLUSION

Our main result has been based on the recently developed second-order semiclassical theory,[33,34] which serves as a rigorous framework for treating such nonlinear effect. In the derivation, we have not made any assumption on the band structure nor the field configuration. So the obtained result is quite general, which is also manifested in the application of our theory to the two distinct model systems.

We have adopted the relaxation time approximation in solving the Boltzmann equation. This approach has been widely used in theoretical studies and in interpreting experimental results.[13,37–39] It has the merit that it is simple enough to allow the derivation of analytical results, yet it still captures the most important effect of scattering, i.e., the tendency to bring the system toward equilibrium. It is remarkable that our intrinsic magnetoconductivity already appears in this simple approximation. To go beyond the relaxation time approximation (e.g. to include possible spin-orbit coupling effects in scattering) would require a detailed evaluation of the collision integral, which would be challenging to proceed analytically unless for very simple models. In future works, it would be an interesting problem to study and estimate such additional corrections to our result.

In conclusion, we have formulated a theory of the magnetoconductivity for non-magnetic metals in the semiclassical regime. We obtain an important new contribution that is missing in previous theories. This intrinsic contribution provides a new mechanism for the violation of Kohler's rule and for a nonzero longitudinal magnetoconductivity. Particularly, it dominates the longitudinal magnetoconductivity in systems without strong Fermi surface anisotropy and topological band-crossings. Furthermore, its value can be positive, hence offering a new origin for positive longitudinal magnetoconductivity besides the chiral anomaly effect. Our result indicates that positive longitudinal magnetoconductivity measured in semiclassical regime alone cannot be regarded as a smoking-gun evidence for the existence of topological band-crossings. The intrinsic contribution generally ex-

ists in three dimensional metals with nontrivial Berry curvatures, and should be taken into account when interpreting experimental results. It may already play an important role behind the puzzling magneto-transport signals observed in recent experiments on $TaAs_2$ and related materials.[30–32,41–43]

Appendix A: Derivation of Eq.(6) in the main text

From the equations of motion in the main text (also see Ref. 33), we find that:

$$\mathcal{D}\dot{\boldsymbol{r}} = \frac{\partial \tilde{\varepsilon}}{\partial \boldsymbol{k}} + \boldsymbol{E} \times \tilde{\boldsymbol{\Omega}} + \left(\frac{\partial \tilde{\varepsilon}}{\partial \boldsymbol{k}} \cdot \tilde{\boldsymbol{\Omega}} \right) \boldsymbol{B} \,, \qquad \text{(A1)}$$

$$\dot{\boldsymbol{k}} = -\boldsymbol{E} - \frac{\partial \tilde{\varepsilon}}{\partial \boldsymbol{k}} \times \boldsymbol{B} - (\boldsymbol{E} \times \tilde{\boldsymbol{\Omega}}) \times \boldsymbol{B} + (\boldsymbol{B} \cdot \boldsymbol{\Omega}_0)(\boldsymbol{v}_0 \times \boldsymbol{B}) \,. \quad \text{(A2)}$$

Based on Eq.(5) in the main text and the above two equations, the distribution function can be obtained as

$$
\begin{aligned}
f - f_0 =& \tau (1 - \boldsymbol{B} \cdot \boldsymbol{\Omega}_0) \boldsymbol{E} \cdot \frac{\partial \tilde{\varepsilon}}{\partial \boldsymbol{k}} f_0' + \tau \left(\frac{\partial \tilde{\varepsilon}}{\partial \boldsymbol{k}} \cdot \boldsymbol{\Omega}_0 \right) (\boldsymbol{E} \cdot \boldsymbol{B}) f_0' \\
&+ \tau^2 \left[\left(\frac{\partial \tilde{\varepsilon}}{\partial \boldsymbol{k}} \times \boldsymbol{B} \cdot \boldsymbol{\partial} \right) (\boldsymbol{E} \cdot \boldsymbol{\partial}) \tilde{\varepsilon} \right] f_0' \\
&- \tau^3 (\boldsymbol{v}_0 \times \boldsymbol{B} \cdot \boldsymbol{\partial})^2 (\boldsymbol{E} \cdot \boldsymbol{v}_0) f_0' \,.
\end{aligned}
\qquad \text{(A3)}
$$

Since the magneto-current we need is $\propto EB^2$, here we drop the terms that contain E^2 or higher power of E.

Combining Eq.(A1) and Eq.(A3), we obtain the current up to third order and $\sim EB^2$. The last term in Eq.(A3) yields the first term in Eq.(6) in the main text. The τ^2 term in Eq.(A3) vanishes because it is odd under time reversal. The other terms can be put into a compact form and yields the second term in Eq.(6) in the main text.

Appendix B: Calculation of shift in chemical potential

Here we outline how one can calculate the shift in the chemical potential due to the second order field correction. Consider the case when the conduction band is separated from the valence band, the electron number n in

the conduction band should be conserved, which means that

$$\int [d\boldsymbol{k}] \mathcal{D} f_0(\tilde{\varepsilon} - \tilde{\mu}) = n \,. \tag{B1}$$

Here we use the short-hand notation $[d\boldsymbol{k}]$ to stand for $\frac{d^3 k}{(2\pi)^3}$. We can write both the corrected band energy and the corrected chemical potential in the expansion form, $\tilde{\varepsilon} = \varepsilon_0 + \varepsilon^{(1)} + \varepsilon^{(2)} + \cdots$ and $\tilde{\mu} = \mu + \mu^{(1)} + \mu^{(2)} + \cdots$, with the superscripts (1) and (2) indicating the order of corrections. The corrections of band energy can be found in Ref. 34.

Expanding the left hand side of Eq. (B1) and counting the order of each term, we obtain the following relations:

$$\int [d\boldsymbol{k}] \boldsymbol{B} \cdot \boldsymbol{\Omega}_0 f_0 = \int [d\boldsymbol{k}](\mu^{(1)} - \varepsilon^{(1)}) f_0'$$

$$\int [d\boldsymbol{k}] \boldsymbol{B} \cdot \boldsymbol{\Omega}^{(1)} f_0 = \int [d\boldsymbol{k}](\mu^{(2)} f_0' - \varepsilon^{(2)})$$

$$- \int [d\boldsymbol{k}] \frac{1}{2}(\mu^{(1)} - \varepsilon^{(1)})^2 f_0'' \,. \tag{B2}$$

Since the shift of chemical potential does not depend on $\boldsymbol{k}$, we can pull it out of the integration. The results are:

$$\mu^{(1)} \int d\varepsilon\, g(\varepsilon) f_0' = \int [d\boldsymbol{k}] \varepsilon^{(1)} f_0' + \int [d\boldsymbol{k}] \boldsymbol{B} \cdot \boldsymbol{\Omega}_0 f_0 \tag{B3}$$

$$\mu^{(2)} \int d\varepsilon\, g(\varepsilon) f_0' = \int [d\boldsymbol{k}] \varepsilon^{(2)} f_0' + \int [d\boldsymbol{k}] \boldsymbol{B} \cdot \boldsymbol{\Omega}' f_0$$

$$+ \frac{1}{2} \int [d\boldsymbol{k}] (\varepsilon^{(1)} - \mu^{(1)})^2 f_0''$$

$$+ \int [d\boldsymbol{k}] \boldsymbol{B} \cdot \boldsymbol{\Omega}_0 \varepsilon^{(1)} f_0' \,. \tag{B4}$$

The shift in chemical potential can be solved from these equations. From Eq. (B3), it is easy to find out that for systems with time reversal symmetry, $\mu^{(1)} = 0$.

Appendix C: Calculation for the model of Weyl semimetals

In the first example considered in the main text, we take the low-energy model of a doped Weyl semimetal. Near the Fermi energy, Weyl semimetals have isolated Weyl points, each described by a Weyl Hamiltonian: $H = \chi v_F \boldsymbol{k} \cdot \boldsymbol{\sigma}$, where $\boldsymbol{\sigma}$ is the vector of Pauli matrices denoting the two crossing bands, $\chi = \pm 1$ gives the chirality, and v_F is the Fermi velocity. We assume that the chemical potential μ is in the conduction band and the magnetic field is along the z-direction. The basic quantities entering our formula include the conduction band energy $\varepsilon = v_f |\boldsymbol{k}|$, the Berry curvature (take $\chi = +1$ here)

$$\boldsymbol{\Omega}_0 = -\frac{v_F^3 \boldsymbol{k}}{2\varepsilon^3}, \tag{C1}$$

the orbital magnetic moment

$$\boldsymbol{m} = -\frac{v_F^3 \boldsymbol{k}}{2\varepsilon^2}, \tag{C2}$$

the energy corrections,

$$\varepsilon^{(1)} = -\frac{v_F^3}{2\varepsilon^2} B \,, \qquad \varepsilon^{(2)} = \frac{v_F^4 B^2}{8\varepsilon^5} v_F^2 (k_x^2 + k_y^2) \,. \tag{C3}$$

and the first order correction to Berry curvature

$$\boldsymbol{\Omega}^{(1)} = \frac{v_F^4 B}{2\varepsilon^6} \left(v_F^2 k_x k_z, v_F^2 k_y k_z, \frac{1}{2}(\varepsilon^2 - 2v_F^2 k_x^2 - 2v_F^2 k_y^2) \right) \,. \tag{C4}$$

Using Eq. (B3) and (B4), we find that the change in chemical potential is $\mu^{(1)} = 0$ and

$$\mu^{(2)} = -\frac{v_F^4}{12\mu^3} B^2 \,. \tag{C5}$$

The zero-magnetic-field conductivity for two pairs of Weyl points can be easily calculated as:

$$\sigma_0 = -2\tau \int \frac{d\boldsymbol{k}}{\pi^3} \frac{v_F^4 k_x^2}{\varepsilon^2} = \frac{2\mu^2}{3\pi^2 v_F} \tau \,. \tag{C6}$$

Plugging the above quantities into our formula (Eqs. (6) and (7) in the main text), we can obtain the results presented in the main text. For example, the transverse magnetoconductivity from the extrinsic contribution is

$$\delta\sigma_{xx}^{\text{ext}} = -\tau^3 \int [d\boldsymbol{k}](v_0)_1 (\boldsymbol{v}_0 \times \boldsymbol{B})_i (\boldsymbol{v}_0 \times \boldsymbol{B})_j \partial_{ij}(v_0)_1$$

$$+ \tau^3 \int [d\boldsymbol{k}](v_0)_1 (\boldsymbol{v}_0 \times \boldsymbol{B})_i \partial_i (\boldsymbol{v}_0 \times \boldsymbol{B})_j \partial_j (v_0)_1] f_0'$$

$$= -\frac{1}{3\pi^2} \tau^3 B^2 v_{\text{F}}^3 = -\sigma_0 (\omega_c \tau)^2 \,, \tag{C7}$$

where $\omega_c = B v_F^2 / \mu$.

Appendix D: Lattice model for the second example

Here we show that the continuum model of the second example in the main text (Eq. (12)) can be realized on a 3D lattice. For example, we take a 3D lattice consisting of 2D honeycomb lattices AA-stacked along the z-direction. Then the lattice model can be constructed as

$$\mathcal{H} = -t \sum_{\langle i,j \rangle, \ell} c_{i,\ell}^\dagger c_{j,\ell} - t_\perp \sum_{i,\ell} \xi_i c_{i,\ell}^\dagger c_{i,\ell\pm1} + M \sum_i \xi_i c_{i,\ell}^\dagger c_{i,\ell}. \tag{D1}$$

Here the subscript (i, ℓ) labels the lattice site: i labels the site location within each honeycomb layer and ℓ is the label of the layer. $\xi_i = \pm 1$ depending on the sublattices in each honeycomb layer. The first term is the intralayer nearest neighboring hopping, the second term is the interlayer hopping, and the last term is an intralayer staggered sublattice potential.

After Fourier transform, one finds that for this lattice model, there are two inequivalent valleys located at the boundary of Brillouin zone connected by time reversal symmetry. It can be written in the form of Eq.(12) in the main text, with the following correspondence:

$$v_F = \frac{3}{2}at, \qquad \Delta = M - 2t_\perp, \qquad m^* = \frac{1}{2t_\perp c^2}. \quad \text{(D2)}$$

Here a is the intralayer nearest neighbor distance, and c is the interlayer distance.

[1] N. W. Ashcroft and N. D. Mermin, *Solid State Physics* (Harcourt, Orlando, 1976).

[2] A. B. Pippard, *Magnetoresistance in Metals* (Cambridge University Press, Cambridge, 1989).

[3] Hereafter we refer to them as transverse and longitudinal magnetoconducitivities, respectively. The transverse magnetoconducitivity should not be confused with Hall conductivity (i.e., the off-diagonal component of conductivity tensor).

[4] P. N. Argyres and E. N. Adams, Phys. Rev. 104, 900 (1956).

[5] P. Goswami, J. H. Pixley, and S. Das Sarma, Phys. Rev. B 92, 075205 (2015).

[6] H. K. Pal and D. L. Maslov, Phys. Rev. B **81**, 214438 (2010).

[7] X. Wan, A. M. Turner, A. Vishwanath, and S. Y. Savrasov, Phys. Rev. B **83**, 205101 (2011).

[8] S. Murakami, New J. Phys. **9**, 356 (2007).

[9] S. M. Young, S. Zaheer, J. C. Y. Teo, C. L. Kane, E. J. Mele, and A. M. Rappe, Phys. Rev. Lett. **108**, 140405 (2012).

[10] B.-J. Yang and N. Nagaosa, Nat. Commun. **5**, 4898 (2014).

[11] S. A. Yang, SPIN **6**, 1640003 (2016).

[12] H. Nielsen and M. Ninomiya, Phys. Lett. B **130**, 389 (1983).

[13] D. T. Son and B. Z. Spivak, Phys. Rev. B **88**, 104412 (2013).

[14] M. M. Vazifeh and M. Franz, Phys. Rev. Lett. **111**, 027201 (2013).

[15] J.-H. Zhou, H. Jiang, Q. Niu, and J.-R. Shi, Chin. Phys. Lett. **30**, 027101 (2013).

[16] A. A. Burkov, Phys. Rev. Lett. **113**, 247203 (2014).

[17] A. A. Burkov, Phys. Rev. B **91**, 245157 (2015).

[18] J. C. W. Song, G. Refael, and P. A. Lee, Phys. Rev. B **92**, 180204(R) (2015).

[19] N. Ramakrishnan, M. Milletari, and S. Adam, Phys. Rev. B **92**, 245120 (2015).

[20] H. Chen, Y. Gao, D. Xiao, A. H. MacDonald, and Q. Niu, arXiv:1511.02557.

[21] B. Z. Spivak and A. V. Andreev, Phys. Rev. B 93, 085107 (2016).

[22] S.-B. Zhang, H.-Z. Lu, and S.-Q. Shen, New J. Phys. **18**, 053039 (2016).

[23] H.-J. Kim, K.-S. Kim, J.-F. Wang, M. Sasaki, N. Satoh, A. Ohnishi, M. Kitaura, M. Yang, and L. Li, Phys. Rev. Lett. **111**, 246603 (2013).

[24] J. Xiong, S. K. Kushwaha, T. Liang, J. W. Krizan, M. Hirschberger, W. Wang, R. J. Cava, and N. P. Ong, Science **350**, 413 (2015).

[25] X. Huang, L. Zhao, Y. Long, P. Wang, D. Chen, Z. Yang, H. Liang, M. Xue, H. Weng, Z. Fang, X. Dai, and G. Chen, Phys. Rev. X **5**, 031023 (2015).

[26] C.-Z. Li, L.-X. Wang, H. Liu, J. Wang, Z.-M. Liao, and D.-P. Yu, Nat. Commun. **6**, 10137 (2015).

[27] R. D. dos Reis, M. O. Ajeesh, N. Kumar, F. Arnold, C. Shekhar, M. Naumann, M. Schmidt, M. Nicklas, and E. Hassinger, New J. Phys. **18**, 085006 (2016).

[28] C.-L. Zhang et al., Nat. Commun. **7**, 10735 (2016).

[29] H. Li, H. He, H.-Z. Lu, H. Zhang, H. Liu, R. Ma, Z. Fan, S.-Q. Shen, and J. Wang, Nat. Commun. **7**, 10301 (2016).

[30] Y. Luo, R. D. McDonald, R. F. S. Rosa, B. Scott, N. Wakeham, N. J. Ghimire, E. D. Bauer, J. D. Thompson, and F. Ronning, Scientific Reports **6**, 27294 (2016).

[31] Y. Li, Z. Wang, Y. Lu, X. Yang, Z. Shen, F. Sheng, C. Feng, Y. Zheng, and Z.-A. Xu, arXiv:1603.04056.

[32] Y. Li, L. Li, J. Wang, T. Wang, X. Xu, C. Xi, C. Cao, and J. Dai, arXiv:1601.02062.

[33] Y. Gao, S. A. Yang, and Q. Niu, Phys. Rev. Lett. **112**, 166601 (2014).

[34] Y. Gao, S. A. Yang, and Q. Niu, Phys. Rev. B **91**, 214405 (2015).

[35] D. Xiao, M.-C. Chang, and Q. Niu, Rev. Mod. Phys. **82**, 1959 (2010).

[36] D. Xiao, J. Shi, and Q. Niu, Phys. Rev. Lett. **95**, 137204 (2005).

[37] I. Sodemann and L. Fu, Phys. Rev. Lett. **115**, 216806 (2015).

[38] J. Xiong, S. Kushwaha, J. Krizan, T. Liang, R. J. Cava, N. P. Ong, Eur. Phys. Lett. **114**, 27002 (2016).

[39] V. Brosco, L. Benfatto, E. Cappelluti, and C. Grimaldi, Phys. Rev. Lett. 116, 166602 (2016).

[40] R. H. McKenzie, J. S. Qualls, S. Y. Han, and J. S. Brooks, Phys. Rev. B **57**, 11854 (1998).

[41] Y. Wang, Q.-H. Yu, P.-J. Guo, K. Liu, and T.-L. Xia, Phys. Rev. B **94**, 041103(R) (2016).

[42] Z. Yuan, H. Lu, Y. Liu, J. Wang, and S. Jia, Phys. Rev. B **93**, 184405 (2016).

[43] Z. Wang, Y. Li, Y. Lu, Z.-X. Shen, F. Sheng, C. Feng, Y. Zheng, and Z.-A. Xu, arXiv:1603.01717.